Probing the Molecular Geometry of Five-Coordinate Vanadyl Complexes with Pulsed ENDOR

Christopher V. Grant,[†] Katherine M. Geiser-Bush,[‡] Charles R. Cornman,[‡] and R. David Britt*,[†]

Departments of Chemistry, University of California, Davis, California 95616, and North Carolina State University, Raleigh, North Carolina 27695-8204

Received August 2, 1999

The pulsed electron paramagnetic resonance (EPR) technique of ^{51}V electron spin echo−electron nuclear double resonance (ESE-ENDOR) has been used to measure the nuclear quadrupole coupling constants of a series of five-coordinate vanadyl complexes containing Schiff base ligands with geometries ranging from distorted square pyramidal to distorted trigonal bipyramidal. Vanadium nuclear quadrupole coupling constants are sensitive to the coordination geometry of the vanadyl ion, and thus sensitive to the structural distortions within this series of complexes. ^{51}V ESE-ENDOR has been shown to be a probe of the coordination geometry of vanadyl complexes. Such a spectroscopic probe should prove useful in the investigation of vanadyl of unknown coordination geometry, such as may be found in the interaction of the vanadyl ion with biomolecules.

Introduction

The discovery of two enzymes that require vanadium for activity, vanadium haloperoxidase and vanadium nitrogenase,[1−3] the capacity of vanadium to modify phosphate metabolism in vitro and in vivo,[4−6] and the ability of vanadium complexes to elicit the effects of insulin in diabetic animals[7−12] has led to great interest in the coordination and redox chemistry of vanadium(V) and vanadium(IV) under biologically relevant conditions.[13,14] For example, it has been shown by protein crystallography that vanadate, $HV(V)O_4^{2-}$, forms stable trigonal bipyramidal complexes (transition state analogues) with protein tyrosine phosphatases (PTPs), thereby strongly inhibiting the PTP-catalyzed dephosphorylation of phosphotyrosine.[15−17] The ability of aqueous vanadyl, $[VO(H_2O)_5]^{2+}$, to inhibit PTPs has not been shown, despite the recent demonstration that vanadyl ion can readily adopt a trigonal bipyramidal coordination geometry.[18] However, vanadyl complexes of catechol-based ligands are potent irreversible inhibitors of PTPs.[19] To fully understand vanadium−ligand−protein interactions, it is important to know the metal oxidation state, the number and identity of coordinating ligands, and the metal coordination geometry.

Electron paramagnetic resonance (EPR) spectroscopy provides a sensitive probe of the electronic and magnetic environment of vanadyl coordination complexes.[20] Hyperfine coupling gives rise to an anisotropic eight-line EPR spectrum for this $I = {}^7/_2$ and $S = {}^1/_2$ spin system. Oxovanadium(IV) complexes are typically five- or six-coordinate, with the oxo ligand defining the *z*-direction of the coordination polyhedron and giving rise to large, approximately axial anisotropy in the hyperfine matrix (**A**). Differences in the four equatorial ligands can give rise to small differences in A_x and A_y,[18] but the identity (or absence) of a sixth ligand trans to the oxo group seems to have little effect on the hyperfine matrix. Since the magnitudes of the components of the hyperfine matrix are sensitive to the electron-donating character of the equatorial ligands, empirical additivity relationships have been developed to take into account their properties for biologically relevant ligands, based on EPR measurements of complexes with known or, in some cases, assumed ligand identity.[20−22] Several workers have used this approach to estimate the identity of the coordinating ligands in

* Corresponding author.
[†] University of California.
[‡] North Carolina State University.

(1) Vilter, H. In *Metal Ions in Biological Systems;* Sigel, H., Sigel, A., Eds.; Marcel Dekker: New York, 1995; Vol. 31, pp 325−362.
(2) Butler, A.; Walker, J. V. *Chem. Rev.* **1993**, *93*, 1937−1944.
(3) Eady, R. R. In *Metal Ions in Biological Systems*; Sigel, H., Sigel, A., Eds.; Marcel Decker: New York, 1995; Vol. 31, pp 363−405.
(4) Crans, D. C. *Comments Inorg. Chem.* **1994**, *16*, 35−76.
(5) Gresser, M. J.; Tracey, A. S.; Stankiewicz, P. *J. Adv. Protein Phosphatases* **1987**, *4*, 35−57.
(6) Stankiewicz, P. J.; Tracey, A. S.; Crans, D. C. In *Metal Ions in Biological Systems*; Sigel, H., Sigel, A., Eds.; Marcel Dekker: New York, 1995; Vol. 31, pp 287−362.
(7) Dubyak, G. R.; Kleinzeller, A. *J. Biol. Chem.* **1980**, *255*, 5306−5312.
(8) Shechter, Y.; Karlish, S. J. D. *Nature* **1980**, *284*, 556−558.
(9) Orvig, C.; Thompson, K. H.; Battel, M.; McNeal, J. H. In *Metal Ions in Biological Systems*; Sigel, H., Sigel, A., Eds.; Dekker: New York, 1995; Vol. 31, pp 575−594.
(10) Shechter, Y.; Meyerovitch, J.; Farfel, Z.; Sack, J.; Bruck, R.; Bar-Meir, S.; Amir, S.; Degani, H.; Karlish, S. J. D. In *Vanadium in Biological Systems*; Chasteen, N. D., Ed.; Kluwer Academic Publishers: Dordrecht, The Netherlands, 1990; pp 129−142.
(11) Goldfine, A. B.; Simonson, D. C.; Folli, F.; Patti, M. E.; Kahn, C. R. *Mol. Cell. Biochem.* **1995**, *153*, 217−231.
(12) Goldfine, A. B.; Folli, F.; Patti, M. E.; Simonson, D. C.; Kahn, C. R. *Can. J. Physiol. Pharmacol.* **1994**, *72*, 11.
(13) Butler, A.; Carano, C. J. *Coord. Chem. Rev.* **1991**, *109*, 61−105.
(14) Rehder, D. *Angew. Chem.* **1991**, *30*, 148−167.
(15) Denu, J. M.; Lohse, D. L.; Vijayalakshmi, J.; Saper, M.; Dixon, J. E. *Proc. Natl. Acad. Sci. U.S.A.* **1996**, *93*, 2493−2498.
(16) Zhang, M.; Zhou, M.; Van Etten, R. L.; Stauffacher, C. V. *Biochemistry* **1997**, *36*, 15−23.
(17) Pannifer, A. D. B.; Flint, A. J.; Tonks, N. K.; Barford, D. *J. Biol. Chem.* **1998**, *273*, 10454−10462.
(18) Cornman, C. R.; Geiser-Bush, K. M.; Rowley, S. P.; Boyle, P. D. *Inorg. Chem.* **1997**, *36*, 6401−6408.
(19) Cornman, C. R.; Boyajian, Y. D.; Ferguson, S. S.; Lohse, D. L.; Dixon, J. E., Submitted for publication.
(20) Chasteen, N. D. In *Biological Magnetic Resonance*; Berliner, L. J., Reuben, J., Eds.; Plenum Press: New York, 1981; Vol. 3, pp 53−119.

10.1021/ic9909173 CCC: $18.00
Published on Web 12/04/1999

vanadyl−peptide and vanadyl−protein systems.[23−29] It has recently been shown that A_z is relatively insensitive to coordination geometry, whereas A_x and A_y are sensitive to geometric perturbations along a square pyramidal-to-trigonal-bipyramidal geometric coordinate.[18] However, a definitive relationship between ligand geometry and A_x and A_y could not be established. Thus, A_z can be used as a first approach to assigning the equatorial ligands, but EPR alone cannot provide full information about coordination geometry.

The technique of ^{51}V electron spin echo-electron nuclear double resonance (ESE-ENDOR) allows for the sensitive measure of ^{51}V nuclear quadrupole coupling constants that have been shown to be sensitive to axial ligand binding trans to the oxo bond of vanadyl complexes and, thus, sensitive to electron density trans to the oxo bond.[30,31] Any chemical or structural change that results in a change of electron density along the VO bond axis should give rise to a change in the nuclear quadrupole coupling constant. As a result, ^{51}V ESE-ENDOR should also be a sensitive probe of the coordination in five-coordinate vanadyl complexes that may adopt geometries between square pyramidal, with little electron density donated trans to the oxo bond by the equatorial ligands, and trigonal bipyramidal, with greater trans electron density donated opposite the oxo bond. This trend has been demonstrated computationally by ab initio density functional theory calculations.[31] In an effort to demonstrate the use of ^{51}V ESE-ENDOR as a geometric probe of five-coordinate vanadyl complexes, a series of complexes have been prepared that range in geometry from distorted square pyramidal to distorted trigonal bipyramidal. This series consists of the following complexes (Figure 1): **[**N,N′-ethylenebis(*o*-*tert*-butyl-*p*-methylsalicylaldiminato)]oxovanadium(IV) (**1**); [*N*,*N*′-propanediylbis(*o*-*tert*-butyl-*p*-methylsalicylaldiminato)]-oxovanadium(IV) (**2**); bis(*N*-methylsalicylaldiminato)oxovanadium(IV); (**3**) bis(*N*-isopropyl-*o*-methylsalicylaldiminato)-oxovanadium(IV) (**4**) bis(*N*-methyl-*o*-*tert*-butyl-*p*-methylsalicylaldiminato)oxovanadium(IV) (**5**).

Experimental Section

The synthesis and characterization of this series of complexes has been described in detail previously.[18] All complexes were dissolved in 1:1 solutions of dried and distilled toluene and methylene chloride. Samples were prepared at approximately 3−5 mM concentration depending on the solubility of the complex. The pulsed EPR/ENDOR spectrometer has been described previously.[32,33] All experiments were carried out at X-band microwave frequencies. Spectra were recorded at a temperature of approximately 15 K by utilizing the Davies ENDOR sequence ($\pi-T-\pi/2-\tau-\pi-\tau-$echo with the rf pulse applied during the time T).[34] Field swept electron spin echo (ESE) EPR spectra were recorded by utilizing the two pulse echo sequence ($\pi/2-\tau-\pi-\tau-$echo), with the echo intensity monitored as a function of magnetic field (Figure 2). Relatively long microwave pulses (100 ns) were used to allow the best possible orientation selection for the Davies ENDOR experiment.[35] ENDOR rf pulses were 18 μs in duration, with a power of 100 W and a frequency increment of 0.1 MHz. In all cases the time T was 2 μs

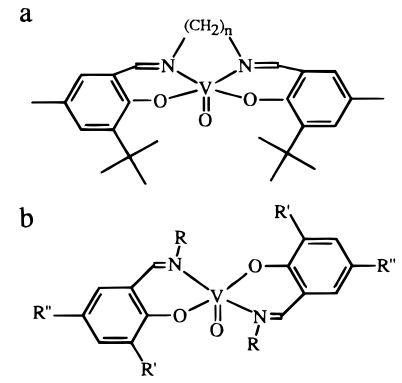

Figure 1. Complexes investigated, where (a) represents complexes **1** and **2**, where $n = 2$ and $n = 3$, respectively, and (b) represents complexes **3**−**5**. For complex **3**, R = CH_3, R′ = H, and R″ = H. For complex **4**, R = isopropyl, R′ = CH_3, and R″ = H. For complex **5**, R = CH_3, R′ = *tert*-butyl, and R″ = CH_3.

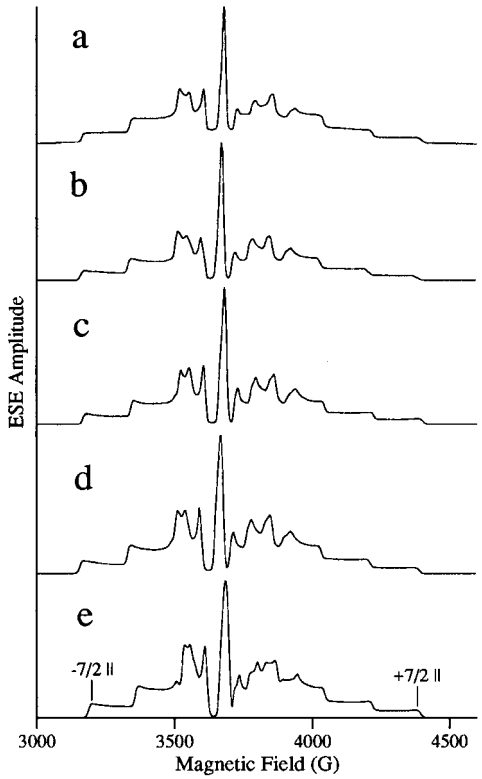

Figure 2. ESE-EPR magnetic field sweep spectra and relevent spectroscopic parameters for (a) complex **1**, $\nu_{mw} = 10.335$ GHz, $\tau = 450$ ns, MW power ∼ 0.25 W, (b) complex **2**, $\nu_{mw} = 10.296$ GHz, $\tau = 500$ ns, MW power ∼ 0.50 W, (c) complex **3** $\nu_{mw} = 10.335$ GHz, $\tau = 420$ ns, MW power ∼ 0.30 W, (d) complex **4**, $\nu_{mw} = 10.296$ GHz, $\tau = 500$ ns, MW power ∼ 0.39 W, and (e) complex **5**, $\nu_{mw} = 10.335$ GHz, $\tau = 450$ ns, MW power ∼ 0.63 W. In all cases $\pi/2$ MW pulse duration = 100 ns and π MW pulse duration = 200 ns.

(21) Holyk, N. H. An Electron Paramagnetic Resonance Study of Model Oxovanadium(IV) Complexes in Aqueous Solution: Correlation of Magnetic Properties with Ligand Type and Metal Chelate Structure. M.S. Thesis, University of New Hampshire, Durham, NH, 1979.
(22) Cornman, C. R.; Zovinka, E. P.; Boyajian, Y. D.; Geiser-Bush, K. M.; Boyle, P. D.; Singh, P. *Inorg. Chem.* **1995**, *34*, 4213−4219.
(23) Chasteen, N. D. In *Metal Ions in Biological Systems*; Sigel, H., Sigel, A., Eds.; Marcel Dekker: New York, 1995; Vol. 31, pp 231−247.
(24) Chasteen, N. D.; DeKoch, R. J.; Rogers, B. L.; Hanna, M. W. *J. Am. Chem. Soc.* **1973**, *95*, 1301−1309.
(25) Cornman, C. R.; Zovinka, E. P.; Meixner, M. H. *Inorg. Chem.* **1995**, *34*, 5099−5100.
(26) Kuwahara, J.; Suzuki, T.; Sugiura, Y. *Biochem. Biophys. Res. Commun.* **1985**, *129*, 368−374.
(27) Chasteen, N. D.; Francavilla, J. *J. Phys. Chem.* **1976**, *80*, 867−871.
(28) Houseman, A. L.; Morgan, L.; LoBrutto, R.; Frasch, W. D. *Biochemistry* **1994**, *33*, 4910−4917.
(29) Houseman, A. L. P.; LoBrutto, R.; Frasch, W. D. *Biochemistry* **1995**, *34*, 3277−3285.
(30) Grant, C. V.; Ball, J. A.; Hamstra, B. J.; Pecoraro, V. L.; Britt, R. D. *J. Phys. Chem. B* **1998**, *102*, 8145−8150.
(31) Grant, C. V.; Cope, W.; Ball, J. A.; Maresch, G. G.; Gaffney, B. J.; Fink, W.; Britt, R. D. *J. Phys. Chem.*, in press.
(32) Sturgeon, B. E.; Britt, R. D. *Rev. Sci. Instrum.* **1992**, *63*, 2187−2192.
(33) Sturgeon, B. E.; Ball, J. A.; Randall, D. W.; Britt, R. D. *J. Phys. Chem.* **1994**, *98*, 12871−12883.
(34) Davies, E. R. *Phys. Lett.* **1974**, *47A*, 1−2.

Table 1. Summary of ENDOR Data and $P_{||}$ Values

complex	$\Delta\nu(+^7/_2)$ (MHz)	$\Delta\nu(-^7/_2)$ (MHz)	$\Delta\Delta\nu$ (MHz)	τ	$P_{||}$ (MHz)
1	16.19	3.16	13.03	0.26	-0.88 ± 0.02
2	15.66	3.85	11.81	0.30	-0.78 ± 0.02
3	15.20	4.42	10.78	0.55	-0.65 ± 0.02
4	14.78	4.89	9.89	0.58	-0.59 ± 0.02
5	14.12	4.68	9.44	0.70	-0.55 ± 0.02

greater than the rf pulse duration. ENDOR field positions were selected such that ESE intensity is monitored at the top edge of the parallel $M_I = \pm^7/_2$ turning points of the ESE-detected EPR spectrum as illustrated in Figure 2e.[30] All ENDOR spectra were fit to Gaussian curves for the determination of the splittings (Table 1). Matrix diagonalization simulations were performed by a FORTRAN computer program of our own construction.[31] Changes in the magnitude of $P_{||}$ greater than 0.02 MHz from the reported values result in simulations with splittings that differ from the experimental splittings by a statisically significant degree. As a result we report these values to ± 0.02 MHz.

Results and Discussion

Data Analysis. ESE-detected magnetic field sweeps of the five complexes are shown in Figure 2; the corresponding ESE-ENDOR spectra obtained at the parallel $M_I = \pm^7/_2$ turning points, and simulations are shown in Figure 3. Our goal is to measure the nuclear quadrupole coupling constant $P_{||}$, where $P_{||} = (3/2)P_{zz} = 3e^2qQ/[4I(2I-1)]$, where q is the electric field gradient along the principal axis of the largest field gradient (the VO bond axis) and Q is the ^{51}V nuclear quadrupole moment (-0.05×10^{-24} cm^2).[36] In our original ^{51}V-ENDOR paper,[30] using perturbation theory, we showed that the $P_{||}$ parameter is proportional to the difference in ENDOR peak splittings obtained at the extreme parallel turning points of the EPR spectra.

More recently, we have developed ENDOR simulation procedures using direct diagonalization of the full Hamiltonian,

$$H = \beta\vec{B}\cdot\mathbf{g}\cdot\vec{S} + \vec{S}\cdot\mathbf{A}\cdot\vec{I} - \beta_n g_n\vec{B}\cdot\vec{I} + \vec{I}\cdot\mathbf{P}\cdot\vec{I} \qquad (1)$$

to obtain more precise values of $P_{||}$.[31] For the five-coordinate complexes **1**−**5**, simulations are performed using the published hyperfine and **g** matrix values.[18] The value of $P_{||}$ is varied until the simulated ENDOR transitions give splittings comparable to those of the experimental ENDOR data obtained at the $M_I = \pm^7/_2$ parallel turning points. The ENDOR splitting frequencies are well simulated (Figure 3) and found to be very sensitive to $P_{||}$ as previously discussed.[30,31] However, absolute frequencies of the ENDOR transitions are not as well simulated. This is likely due to the uncertainty in the determination of **g** and **A** matrix values[18] and the possibility that small rotations of the hyperfine interaction with respect to the **g** matrix may exist. Matrix rotations are not considered in this work because of the difficulty in estimating the coincidence of these interactions without performing EPR experiments at multiple microwave frequencies.[37] The asymmetry parameter η is not reported here because this parameter is not estimated reliably from these simulations due to the lack of sensitivity that the ^{51}V ENDOR frequencies exhibit as a function of η.[31]

(35) Hoffman, B. M.; DeRose, V. J.; Doan, P. E.; Gurbiel, R. J.; Houseman, A. L. P.; Telser, J. In *Biological Magnetic Resonance*; Berliner, I. J., Reuben, J., Eds.; Plenum: New York, 1993; Vol. 13, pp 151−218.
(36) Weltner, W., Jr. *Magnetic Atoms and Molecules*; Dover: New York, 1983; p 342.
(37) Garner, C. D.; Collison, D.; Mobbs, F. E. In *Metal Ions in Biological Systems*; Sigel, H., Sigel, A., Eds.; Marcel Dekker: New York, 1995; Vol. 31, pp 617−670.

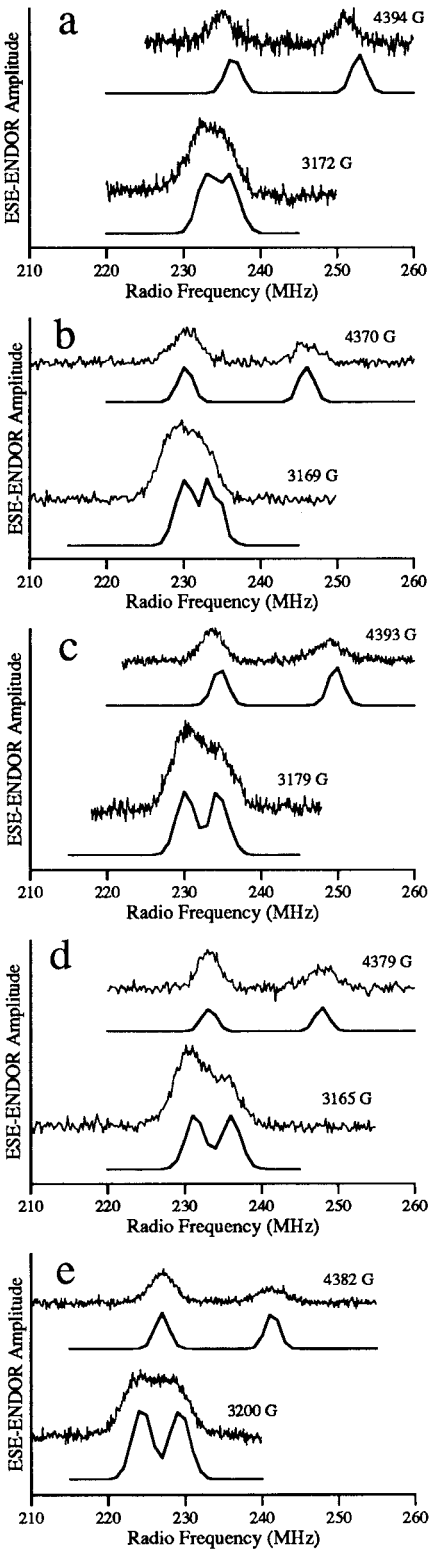

Figure 3. ^{51}V ESE-ENDOR spectra and relavent spectroscopic parameters for (a) complex **1**, $\nu_{mw} = 10.335$ GHz, $\tau = 450$ ns, MW power ~ 0.25 W, (b) complex **2**, $\nu_{mw} = 10.296$ GHz, $\tau = 500$ ns, MW power ~ 0.50 W, (c) complex **3**, $\nu_{mw} = 10.335$ GHz, $\tau = 420$ ns, MW power ~ 0.30 W, (d) complex **4**, $\nu_{mw} = 10.296$ GHz, $\tau = 500$ ns, MW power ~ 0.39 W, and (e) complex **5**, $\nu_{mw} = 10.335$ GHz, $\nu = 450$ ns, MW power ~ 0.63 W. In all cases $\pi/2$ MW pulse duration $= 100$ ns, π MW pulse duration $= 200$ ns, ENDOR rf pulse duration $= 18$ μs, $T = 20$ μs, and rf power ~ 100 W. Matrix diagonalization simulations are shown as smooth curves. Field positions for the top ($+^7/_2$ parallel) and the bottom ($-^7/_2$ parallel) traces for each complex are included.

Chart 1. Illustration of a Vanadyl Complex and the Definition of the Value τ, which Describes the Geometry

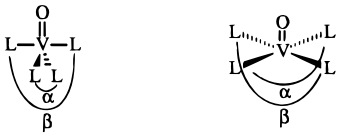

$$\tau = (\beta - \alpha) / 60$$

The stuctures of the studied complexes are parametrized by the value τ which is illustrated in Chart 1. A τ value of 0 is reached in the limit of perfect square pyramidal geometry and a value of 1 in the trigonal bipyramidal limit. Table 1 summarizes the calculated quadrupole coupling constants for this series of complexes. Complex **1** is best described as distorted square pyramidal **(**$\tau = 0.26$), and $P_{||}$ is of the largest magnitude for the series at -0.88 ± 0.02 MHz. As τ increases for complexes **2**−**4**, the magnitude of $P_{||}$ decreases, from -0.78 ± 0.02 MHz for complex **2 to** -0.65 ± 0.02 MHz for complex **3** and -0.59 ± 0.02 MHz for complex **4**, with τ values of 0.30, 0.55, and 0.58, respectively. Complex **5** has the greatest τ value ($\tau = 0.70$) and has a molecular geometry that would be best described as distorted trigonal bipyramidal. $P_{||}$ is measured as -0.55 ± 0.02 MHz, the lowest magnitude quadrupole coupling constant for this series of complexes.

Interpretation of Data. The nuclear quadrupole coupling constant $P_{||}$ is sensitive to electron density along the oxo-bond axis, and the magnitude of the quadrupole interaction is dependent on the electric field gradient at the vandium nucleus. Neglecting all contributions to the electric field gradient besides those that occur as the result of ligands donating electron density into the d orbitals of the vanadium ion, one can conclude that the oxo bond establishes the majority of the electric field gradient along the oxo-bond axis. In our initial report,[30] we investigated VO(salen) and VO(salen) coordinated axially by pyridine. These two complexes give $P_{||}$ values of -0.9 and -0.7 MHz, respectively (noting that these values have been estimated by matrix diagonalization, our previously published values were estimated by perturbation theory). In this previous work[30] we concluded that the nuclear quadrupole coupling constants are sensitive to axial ligation and rather insensitive to equatorial donors with respect to the exchange of nitrogen and oxygen donors for the series of complexes studied. The nuclear quadrupole coupling constant is also sensitive to the structural distortions of this series of five-coordinate complexes. In the case of complex **1**, there is very little electron density donated trans, or opposite the oxo bond. In the case of complex **5** the distorted trigonal bipyramidal geometry allows for an increase in electron density donated opposite the oxo bond and thus diminishes the electric field gradient established by the oxo bond. As illustrated in the $P_{||}$ vs τ graph (Figure 4), as τ increases, the amount of electron density donated trans to the oxo bond increases, thus diminishing the magnitude of the nuclear quadrupole interaction. The linearity of this plot indicates that the electric field gradient along the vanadyl oxo-bond axis decreases with a linear trend as a function of the τ parameter, which quantifies the degree of distortion from square pyramidal to trigonal bipyramidal geometry (slope $= 0.71$ $P_{||}$ (MHz)/τ; y-intercept $= -1.03 P_{||}$ (MHz)). Though all compounds reported here have two O and two N equatorial ligands, we note that complexes **1** and **2** have a different N vs O ligation symmetry compared to compounds **3**−**5**. This is not reflected in the simple geometrical τ parameter, which provides a good linear fit to the reported splittings, so we would argue that the ligand permutations do not appreciable affect $P_{||}$. Thus ^{51}V ESE-ENDOR provides a sensitive measure of the structural distortions found in this series of complexes. Due to the size of these transition metal complexes, we have not yet performed density functional calculations of nuclear quadrupole coupling parameters as we recently did for the aqueous vanadyl complex.[31] This is a target of future research.

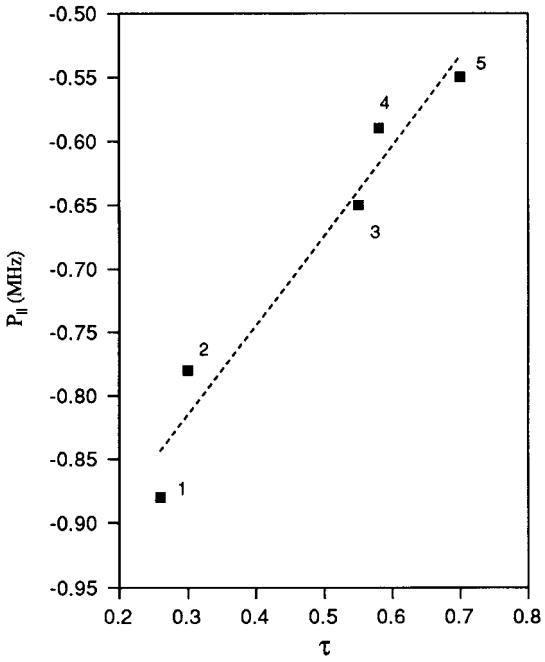

Figure 4. Graph of $P_{||}$ vs τ for complexes **1**−**5**. The dashed line is a linear fit to the data with the following fit parameters: slope $= 0.71$ $P_{||}$ (MHz)/τ; y-intercept $= -1.03$ $P_{||}$ (MHz).

Conclusion

^{51}V nuclear quadrupole couplings measured with the technique of ^{51}V ESE-ENDOR have been shown to be sensitive to the ligand geometry changes in the series of five complexes studied that range from distorted square pyramidal to distorted trigonal bipyramidal. The measured nuclear quadrupole coupling constant $P_{||}$ linearly decreases in magnitude as the value of the distortion parameter τ increases, resulting in electron density being donated opposite the oxo bond and, thus, diminishing the electric field gradient established at the vanadium nucleus. The linearity of the $P_{||}$ vs τ plot indicates that ^{51}V ESE-ENDOR is a potentially useful technique for the investigation of unknown coordination geometries of the vanadyl ion, such as vanadyl adducts of biological molecules.

Acknowledgment. This work was supported by grants from the NSF (CHE 9702873 to C.R.C.) and the NIH (GM48242 to R.D.B.).

IC9909173